International Conference on Nuclear Data for Science and Technology 2007
DOI: 10.1051/ndata:07242

^{235m}U and ^{235}U neutron-induced fission

V.M. Maslov

Joint Institute for Nuclear and Energy Research, 220109 Minsk-Sosny, Belarus

Abstract. Neutron cross sections of ^{235}U and ^{235m}U are obtained via Hauser-Feshbach model calculations. The cross section differences are attributed to the spectroscopic properties of the transition states at saddle deformations of ^{236}U and the coupling strengths of the deformed optical potential for the target spin values $7/2^-$ and $1/2^+$. The ^{235m}U(n,f) cross section at $E_n \lesssim 0.1$ MeV depends on the position of octupole states at outer saddle, being ~2 times lower than that of ^{235}U(n,f) at $E_n \sim 1$ keV. The capture-to-fission ratio of ^{235}U and ^{235m}U is affected at $E_n \lesssim 0.1$ MeV, being ~2 times higher for the latter at $E_n \sim 1$ keV. ^{235}U(n,xn) reaction cross sections and prompt fission neutron spectra (PFNS) are dependent on the emissive fission chances contributions to the observed $\sigma(n, F)$ of ^{235}U, which are much different from the latest evaluations of ENDF/B and JEFF. The role of exclusive pre-fission (n,xnf) neutron spectra for the ^{235}U(n,F) PFNS description and prediction of PFNS for ^{239}Pu(n,F) is exemplified.

1 Introduction

Notwithstanding the years of experimental and theoretical efforts, the evaluated capture and neutron inelastic scattering cross sections of ^{235}U in major data libraries differ a lot. Since these cross sections are obtained via Hauser-Feshbach model calculations, the part of the differences might be attributed to the spectroscopic properties of the transition states at inner and outer saddles deformations of fissioning ^{236}U. Another source of discrepancies are the coupling strengths of the deformed optical potential. These two factors would influence the yield via inelastic neutron scattering of the 77 eV $1/2^+$ isomer ^{235m}U and ^{235m}U(n,f) cross section, which might be measured soon [1]. Though the relative contributions of transition states to the fission cross section are much affected by the target spin value ($7/2^-$ for ^{235}U and $1/2^+$ for ^{235m}U) and relative heights of the inner and outer fission barrier humps [2], the fair description of ^{235}U(n,f) ($7/2^-$), ^{237}U(n,f) ($1/2^+$) [3] and ^{233}U(n,f) ($5/2^+$) allows predict reliably ^{235m}U(n,f). We will investigate the influence of the spectroscopic and coupling factors on the predicted ^{235}U and ^{235m}U fission, capture and inelastic scattering cross sections at 1 keV $\lesssim E_n \lesssim$ 5 MeV.

^{235}U(n,xn) reaction cross sections and PFNS are affected by the emissive fission chances distribution $\beta_x = \sigma(n, xnf)/\sigma(n, F)$ of ^{235}U(n,F). Present β_x are based on consistent description of the cross section data base and PFNS, differs from the evaluations of ENDF/B [4] and JEFF [5].

2 First chance fission

The direct excitation of the ^{235}U $K^\pi = 7/2^-$ band levels is calculated within rigid rotator model, 4 levels $7/2^-$-$9/2^-$-$11/2^-$-$13/2^-$ are assumed coupled, while in case of ^{235m}U, levels $1/2^+$-$3/2^+$-$5/2^+$-$7/2^+$ are coupled. We adopted here the optical potential parameters obtained by fitting total cross section data, angular distributions and s-wave strength function [6]. The step-like structure in ^{235}U(n,f) reaction cross section at $E_n \sim 1$ MeV (see fig. 1) was shown to be a consequence of

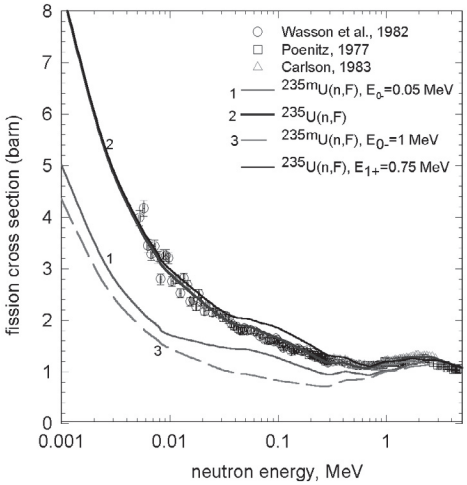

Fig. 1. ^{235}U(n,f) cross section.

threshold excitation of two-quasi-particle states in fissioning ^{236}U nuclide and three-quasi-particle configurations in odd nuclide ^{235}U [7]. The value of the ^{236}U outer fission barrier value is fixed by the description of that structure. Collective states of ^{236}U nuclide are assumed to have a rotational bands with a rotational constant $F_0/\hbar^2$, dependent upon saddle deformations. Inner saddle A is assumed to be axially and mass symmetric, while outer saddle axially symmetric but mass asymmetric. The latter peculiarity leads to the lowering of the negative parity octupole vibration bands at deformations of the outer saddle B. At excitations within a pairing gap, the ^{235}U(n,f) and ^{235m}U(n,f) fission cross sections are defined by the collective levels at saddle deformations. They are much sensitive to the lowering at outer saddle deformations (due to the mass asymmetric deformation) of the octupole band $K^\pi = 0^-$ levels.

The collective levels of $^{232-238}$U at g.s. deformations, lying within the pairing gap, were interpreted within a soft rotator model [8]. The structures of the quadrupole transversal γ-vibration $K^\pi = 0_2^+$, anomalous rotational γ-vibration $K^\pi = 2_1^+$, quadrupole longitudinal β-vibration $K^\pi = 0_3^+$ bands as well

Table 1. Transition spectra band-heads of ^{236}U nuclide.

inner saddle		outer saddle		^{238}Ug.s. deformation	
K^π	E_{K^π}, MeV	K^π	E_{K^π}, MeV	K^π	E_{K^π}, MeV
0^+_1	0.0	0^+_1	0.0	0^+_1	0.0;
0^+_2	0.65	0^+_2	0.65	0^+_2	0.9257 (γ-vib.);
2^+_1	0.7	2^+_1	0.7	2^+_1	1.0603 (γ-vib.);
0^-_1	0.4	0^-_1	0.05	0^-_1	0.6801 (oct-vib.);
1^-_1	0.4	1^-_1	0.05	1^-_1	0.9308 (oct-vib.);
0^+_3	0.7	0^+_3	0.7	0^+_3	0.993 (β-vib.);
1^+	0.95	1^+	0.95	1^+	

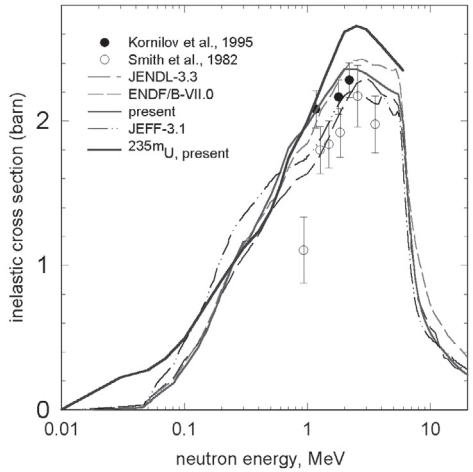

Fig. 2. ^{235}U(n,n') cross section.

as first octupole $K^\pi = 0^-_1$ band levels were analyzed with the deformed non-axial, soft to quadrupole β- and γ-vibrations rotator. The excitation energies of the members of the even-parity collective bands $K^\pi = 0^+_1$, 0^+_2, 0^+_3, 2^+_1 and the first octupole band $K^\pi = 0^-_1$, were reproduced. With increase of the quadrupole deformations, corresponding to stretching of the fissioning nucleus, the relative positions of the collective band structure of ^{236}U may change, just as they change for neighbor ^{232,234,236,238}U or ^{232}Th nuclides [9]. We will assume that the structures of the positive parity collective levels at saddle and g.s. deformations are similar, only actual positions might be slightly lowered. The inclusion of $K^\pi = 0^+_2$ and $K^\pi = 0^+_3$ into the transition states scheme may seem questionable [2], however, without these states it is impossible to reproduce the data trends of ^{235}U(n,f) and ^{233}U(n,f) for incident neutron energies below ~1 MeV [10]. The levels of the $K^\pi = 0^-_1$ band are most sensitive to the octupole deformations, which slightly influence also the positions of other collective band levels. The $K^\pi = 1^+_1$ collective band levels are "excited" by the s-wave neutrons, incident on ^{235m}U [2]. Fission via high lying $K^\pi = 1^+_1$ transition states influences ^{235}U(n,f) fission cross section in the range 40 keV $\lesssim E_n \lesssim$ 400 keV (fig. 1) and ^{239}Pu(n,f) in the range ($E_n \lesssim$ 100 keV). It allows to fix $K^\pi = 1^+_1$ position and predict ^{237}U(n,f) [3]. At outer (higher) saddle of the fission via $K^\pi = 1^+_1$ transition states would be sub-barrier. We construct the discrete transition spectra of ^{236}U up to ~1.3 MeV, using the band heads $K^\pi = 0^+_1$, $K^\pi = 0^+_2$ and $K^\pi = 0^+_3$ $K^\pi \backsimeq 2^+_1$, $K^\pi = 0^-_1$ $K^\pi = 1^+_1$ and $K^\pi = 1^-_1$, shown in table 1.

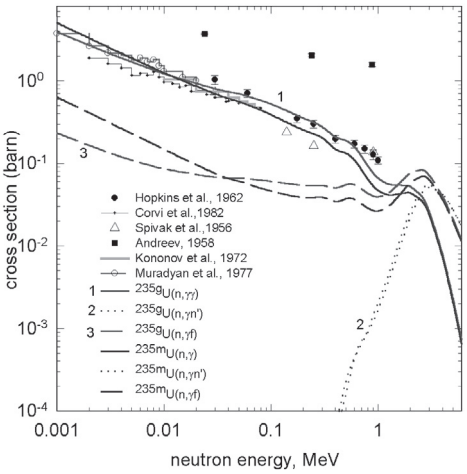

Fig. 3. ^{235}U capture cross section.

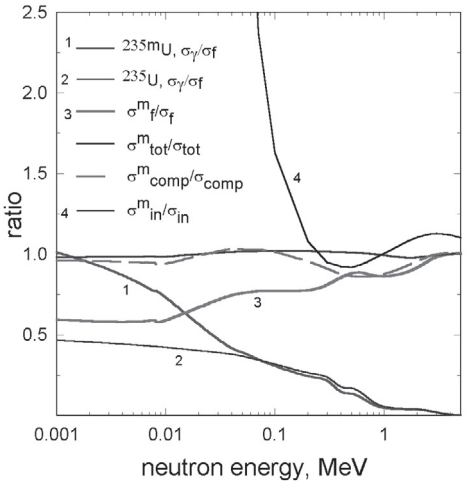

Fig. 4. ^{235m}U and ^{235}U cross section ratios.

The influence of the target spin on the fission cross sections of ^{235}U(n,f) and ^{235m}U(n,f) is shown on figure 1. For ^{235m}U(n,f) the estimate of the fission cross section in the range 10 keV $\lesssim E_n \lesssim$ 100 keV is defined by the lowering of the $K^\pi = 0^-_1$ and $K^\pi = 1^-_1$ bands for the outer fission barrier, since the p-wave neutrons excite here the compound states with negative parity. Similar shape, observed experimentally in surrogate reactions [11] for ^{231}Th(n,f) ($I^\pi = 3/2^+$) was interpreted in [12].

Figure 2 shows that our estimate of ^{235}U(n,n') cross section is consistent with data [13], but severely overshoots data [14]. The ^{235m}U(n,n′) cross section estimate is much higher than that of ^{235}U(n,n') below $E_n \sim$ 200 keV and above $E_n \sim$ 1 MeV. In the lower range it is due to decreased fission competition, while in MeV-range it is an entrance/exit neutron channel effect.

Figure 3 shows the description of capture data [15–20] for ^{235}U(n,γ) and prediction of ^{235m}U(n,γ) cross section. The target spin differences strongly influences the (n,γf) competition to capture reaction (n,$\gamma\gamma$). Most strongly the transition sates spectroscopy influences the capture/fission ratio at $E_n \leq$ 30 keV (fig. 4). Figure 4 shows also the ratios of fission, inelastic scattering and total cross sections for ^{235}U and ^{235m}U.

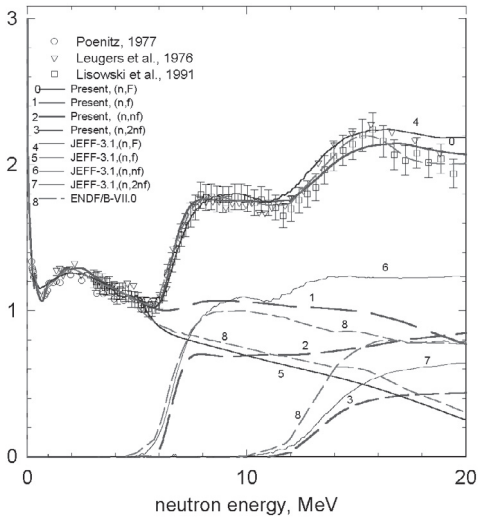

Fig. 5. ^{235}U(n,F) cross section.

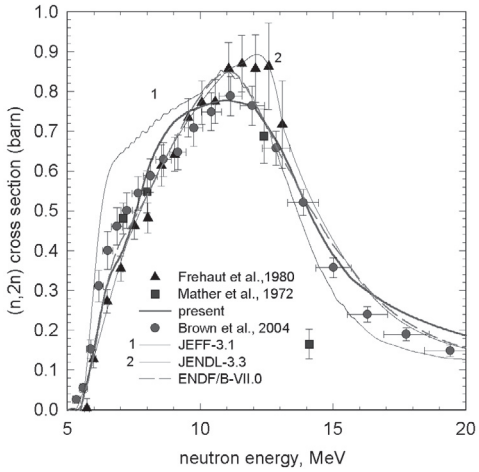

Fig. 6. ^{235}U(n,2n) reaction cross section.

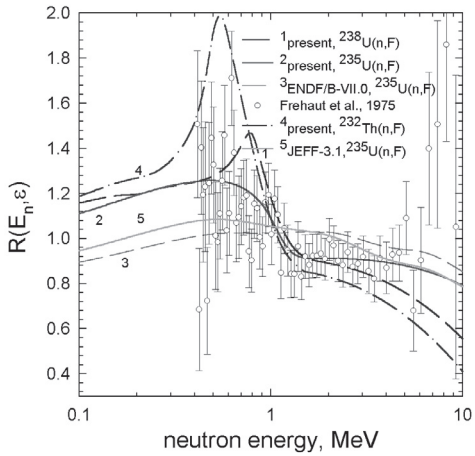

Fig. 7. PFNS, $E_n = 7$ MeV relative to maxwellian $\langle E \rangle = 2.136$ MeV.

3 Emissive fission

The few-quasiparticle effects in even nuclides are important also for modelling of ^{235}U(n,2n) and ^{235}U(n,nf) reaction cross sections. Fission cross section data of ^{235}U(n,F) up to $E_n \sim 20$ MeV are compared with evaluations on figure 5. Data [21–23] for ^{235}U(n,F) reaction were described simultaneously with ^{235}U(n,2n) (fig. 6) and ^{235}U(n,3n) reaction cross section data [24–26]. The pre-equilibrium first neutron contribution is confirmed by (n,2n) data [26], the relevant model parameters were fixed by fitting data on ^{238}U(n,2n) and ^{232}Th(n,2n) [12]. The most important point is that the ^{235}U(n,2n) cross section is consistent with fission probabilities P_f of ^{235,234}U and observed ^{235}U(n,F) fission cross section. Predicted fission chances distribution is strongly discrepant with the distributions of ENDF/B [4] and JEFF [5]. For $E_n \geq E_{n,nf}$, first-chance fission cross section of ^{235}U(n,f) exhibits similar trend as predicted for ^{238}U(n,F) and ^{232}Th(n,F) reactions [12,27,28] and could be considered unambiguous. The same conclusion was drawn in case of n + ^{238}U and n + ^{232}Th data analysis [12,27, 28]. The unambiguity of the fission chances for ^{238}U(n,F) [3] is granted by surrogate data for ^{237}U(n,F) [29,30]. It might be argued that estimates of multiple-chance fission contributions, different from ours, shown on figure 5, would either deteriorate consistent description of ^{235}U(n,F), ^{235}U(n,2n) and ^{235}U(n,3n) or ^{234}U(n,f) and ^{233}U(n,f) cross sections.

4 Prompt fission neutron spectra

For modelling of PFNS we use exclusive (n,*x*nf) neutron spectra, which provide consistent ^{235}U data description. The energy dependence of PFNS of ^{235}U(n,F) reaction for prompt fission neutron energies $\varepsilon \lesssim E_{th} \sim E_n - B_f$ resembles the shape of the P_f of ^{235}U nuclide, B_f being effective fission barrier value of ^{235}U. The energy dependences of PFNS for ^{238}U and ^{232}Th for $\varepsilon \lesssim E_{th}$ resemble the shape of P_f of ^{238}U or ^{232}Th nuclides, respectively [27,28]. The strong point of ^{235}U(n,F) data analysis is that P_f of the residual nuclides ^{235}U and ^{234}U are well investigated via ^{234}U(n,f) and ^{233}U(n,f) reactions. Increase of the contributions of ^{235}U(n,nf) or ^{235}U(n,2nf) to the ^{235}U observed fission cross section, actually adds more soft neutrons to the calculated PFNS spectra, but never fills the gap between PFNS data [31] at $E_n = 7$ MeV and model calculations [4,32,33] (see fig. 7). The effect of (n,nf) neutrons is the strongest for ^{232}Th(n,F) reaction. It was shown in [6] that similar discrepancies are observed at $E_n = 14.7$ MeV when compared to recent ^{235}U(n,F) PFNS data [34,35].

Modelling of the spectra of neutrons, emitted from the fission fragments [36], appears to be rather crude, however it nicely reproduces measured PFNS for ^{232}Th(n,F) and ^{238}U(n,F) [27], ^{235}U(n,F) [6] and might be used for PFNS prediction for the nuclides with various fissilities [37–40]. Figure 8 shows the comparison of the $\langle E \rangle$ of PFNS for ^{232}Th, ^{238}U, ^{235}U and ^{239}Pu target nuclides, calculated with the present model, with calculations by Madland [33] for ^{238}U(n,F), ^{235}U(n,F) and ^{239}Pu(n,F) [4]. Measured data for ^{235}U and ^{239}Pu are shown for thermal neutrons and $E_n = 1.5$ MeV. For ^{239}Pu(n,F) there is no other reliable measured data. For ^{238}U only data in the vicinity of the ^{238}U(n,nf)

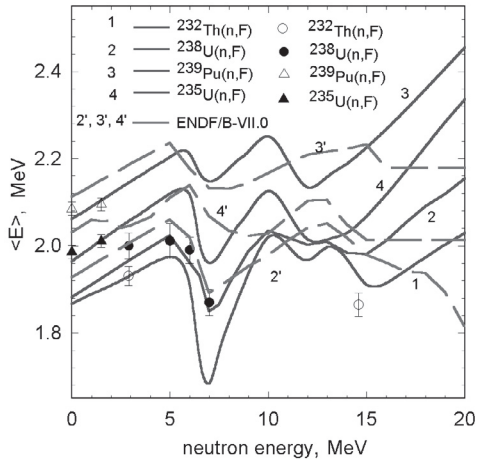

Fig. 8. ⟨E⟩ of PFNS for ^{232}Th(n,F), ^{238}U(n,F), ^{235}U(n,F) and ^{239}Pu(n,F) (solid lines), dashed lines 2', 4', 3'– [4,33] for ^{238}U(n,F), ^{235}U(n,F) and ^{239}Pu(n,F), respectively; △ – ^{239}Pu(n,F) [41,42], ▲ – ^{235}U(n,F) [41,42]; ● –^{238}U(n,F) [35,43–45]; ○ –^{232}Th(n,F) [35,43].

reaction threshold are shown, for ^{232}Th all available data are shown. In our calculations there is strict correlation of the "dips" in PFNS average energies with emissive fission contributions to the observed fission cross sections. The pre-fission neutrons influence is the strongest in case of ^{232}Th and weakest in case of ^{239}Pu. That peculiarity is not due to the fact, that ^{239}Pu(n,F) fission fragments are most heated, but with the highest contribution of the first chance fission to the ^{239}Pu(n,F) fission cross section. That is a convincing illustration of the importance of the precise description of the observed PFNS for the investigation of sharing of the excitation energy between the fission fragments and pre-fission neutrons.

5 Conclusions

Influence of the transition state spectroscopy on ^{235m}U(n,f) and ^{235}U(n,f) cross sections is shown to be important for the capture and inelastic scattering cross section prediction. Combined effect of p-wave neutrons and $K^\pi = 0_1^-$ octupole band at outer saddle of ^{236}U is predicted for ^{235m}U(n,f). The position of $K^\pi = 1^+$ band, important for the ^{235m}U(n,f) cross section prediction at $E_n \leq 500$ keV is fixed by ^{235}U(n,f), ^{237}U(n,f) and ^{239}Pu(n,f) cross section description. Proposed fission chances distribution is shown to be consistent with ^{235}U(n,2n) data and systematics trends. The proposed modifications of inelastic neutron scattering on ^{235}U and PFNS might contribute to further decrease of the discrepancies still observed in simulation of critical assemblies [4]. The role of exclusive (n,xnf) neutron spectra in ^{235}U(n,F) PFNS description and prediction of PFNS for ^{239}Pu(n,F) is demonstrated.

The support of International Atomic Energy Agency is acknowledged.

References

1. D. Rochman et al., Nucl. Instrum. Meth. A **550**, 397 (2005).
2. J.E. Lynn, At.C. Hayes, Phys. Rev. C **67**, 014607 (2003).
3. V.M. Maslov, Phys. Rev. C **72**, 044607 (2005).
4. M.B. Chadwick et al., Nucl. Data Sheets **107**, 2931 (2006).
5. *The JEFF-3.1 Nuclear Data Library*, edited by A. Koning, R. Forrest, M. Kellett e.a., NEA No. 6190, OECD.
6. V.M. Maslov et al., Nucl. Phys. A **760**, 274 (2005).
7. A.V. Ignatyuk, V.M. Maslov, Phys. At. Nucl. **54**, 392 (1991).
8. V.M. Maslov et al., Nucl. Phys. A **764**, 212 (2006).
9. V.M. Maslov et al., in *Proc. International Conference on Nuclear Data for Science and Technology, Tsukuba, 2001*, p. 148.
10. V.M. Maslov et al., INDC(BLR)-18 (2003), IAEA, Vienna.
11. W. Younes, H.C. Britt, Phys. Rev. C **68**, 034610 (2003).
12. V.M. Maslov, Nucl. Phys. A **743**, 236 (2004).
13. N.V. Kornilov et al., Nucl. Sci. Eng. **120**, 55 (1995).
14. A.B. Smith et al., in *Proc. International Conference on Nuclear Data for Science and Technology, Antwerpen, 1982* (1983), p. 39.
15. J.C. Hopkins, B.C. Diven, Nucl. Sci. Eng. **12**, 169 (1962).
16. F. Corvi et al., NEANDC(E)-232, 5 (1982).
17. B. Spivak et al., Sov. J. At. Energy **1**, 26 (1956).
18. V.M. Andreev, Sov. J. At. Energy **4**, 247 (1958).
19. V.M. Kononov et al., Sov. J. At. Energy **32**, 85 (1972).
20. G.V. Muradyan et al., in *Fourth All-Union Conf. on Neutron Physics, Kiev, 1977*, Vol. 3 (Moscow, 1978), p. 119.
21. W.P. Pönitz, Nucl. Sci. Eng. **64**, 894 (1977).
22. P.W. Lisowski et al., in *Proc. Specialists' Meeting on Neutron Cross Section Standards for the Energy Region above 20 MeV, Uppsala, 1991* (OECD, Paris, 1991), p. 177.
23. B. Leugers et al., in *Proc. NEANDC/NEACRP Spec. Meeting on Fast Neutron Fission Cross Sections of ^{233}U, ^{235}U, ^{238}U and ^{239}Pu. ANL, 1976* (ANL-76-90, 1976), p. 183.
24. J. Frehaut et al., Nucl. Sci. Eng. **74**, 29 (1980).
25. D.C. Mather et al., AWRE 072/72, 1972.
26. D.A. Brown et al., LLNL Report, 2004 (in press).
27. V.M. Maslov et al., Phys. Rev. C **69**, 034607 (2004).
28. V.M. Maslov et al., Eur. Phys. J. A **18**, 93, 2003.
29. C. Plettner et al., Phys. Rev. C **71**, 051602(R) (2005).
30. J.T. Burke et al., Phys. Rev. C **73**, 054604 (2006).
31. J. Frehaut, A. Bertin, R. Bois, in *Third All-Union Conf. on Neutron Physics, Kiev, 1975*, Vol. 5 (Moscow, 1975), p. 349.
32. D.C. Madland, J.R. Nix, Nucl. Sci. Eng. **81**, 213 (1982).
33. D.G. Madland, Nucl. Phys. A **772**, 113 (2006).
34. T. Ethvignot et al., Phys. Rev. Lett. **94**, 052701 (2005).
35. G.N. Lovchikova et al., in *Proceedings of the XIV International Workshop on Nuclear Fission Physics, Obninsk, 2000* (Obninsk, 2000), p. 72.
36. N.V. Kornilov et al., Phys. At. Nucl. **62**, 173 (1999).
37. V.M. Maslov et al., in *Proc. International Conference on Nuclear Data for Science and Technol., Santa Fe, 2004* (AIP, 2004), p. 191.
38. V.M. Maslov, VANT, Ser. Fission Reactors **2**, 33 (2006).
39. V.M. Maslov, Atomnaya Energiya (2007) (in press).
40. V.M. Maslov, Phys. At. Nucl. (2007) (in press).
41. B.I. Starostov et al., VANT, Ser. Nuclear Constants **3**, 16 (1985).
42. G.N. Lovchikova et al., Phys. At. Nucl. **62**, 1551 (1999).
43. G.S. Boykov et al., Phys. At. Nucl. **53**, 628 (1991).
44. G.S. Boykov et al., Ann. Nucl. Energy **21**, 585 (1994).
45. G.N. Lovchikova et al., Phys. At. Nucl. **67**, 1246 (2004).